Cool Stars, Stellar Systems and the Sun
ASP Conference Series, Vol. 154, 1998
eds. R. A. Donahue and J. A. Bookbinder

Theoretical Basis of Stellar Activity Cycles

Axel Brandenburg

Department of Mathematics, University of Newcastle, NE1 7RU, UK

Abstract:

Numerical simulations of hydromagnetic turbulence in the presence of shear and/or convection have given us new clues as to how the solar dynamo might work. Simulations suggest that there is significant large-scale magnetic field generation at the bottom of the convection zone, where the radial shear is largest. The nature of the dynamo in the simulations seems to be qualitatively similar to an $\alpha\Omega$-dynamo. However, the origin of the effective α in the simulations is not thermal convection, but magnetobuoyancy and magnetic shear instabilities. This results in a negative α-effect. The efficiency of the α-effect on the one hand, and losses on the other, should increase as the field strength increases. It is argued that this could lead to an increasing ratio between cycle and rotation frequency with increasing field strength, as is indicated by the stellar cycle data of Baliunas and collaborators. Furthermore, to explain the cycle data for active stars one has to invoke another, as yet unknown, type of magnetic instability for which both α and the flux loss are abruptly reduced above a certain field strength. However, details of this speculation are still unclear.

1. Introduction

Solar and stellar activity is usually explained as the result of some kind of an $\alpha\Omega$-dynamo. Problems arise, however, both on observational and theoretical grounds. In other words, not only does a model need to reproduce the observations, but it also has to be consistent and theoretically sound. In fact, at present there is no good model of the solar dynamo. Solutions have been offered to solve some of the problems. For example, the correct solar butterfly diagram has been reproduced by assuming a negative sign of α in the northern hemisphere. Qualitatively, a negative α could arise at the bottom of the convection zone, because there the downward moving fluid must overturn and therefore expand. This changes the sign of the helicity locally, and this could also change the sign of α. However, in the bulk of the convection zone the sign of α should still be positive and this would yield the wrong direction of field migration. Thus, one has to assume *ad hoc* that α vanishes in the bulk of the convection zone; see Rüdiger & Brandenburg (1995) for a recent paper on this approach. Even then there remain a number of things to be "adjusted", for which there is not much theoretical justification.

On the theoretical side there are a variety of problems. Sophisticated three-dimensional simulations of convective dynamo action in spherical shells by Gilman (1983) and Glatzmaier (1985) did produce dynamo action, but there the

field migrated in the wrong direction and the resulting differential rotation was approximately constant on cylinders, which is not consistent with helioseismology. Such simulations leave little room for maneuvering, because of the absence of suitable free parameters. On the other hand, in mean-field dynamo theory (e.g., Moffatt 1978) one is used to manipulate quite freely various coefficients to make things work. We return to this further below.

In the present paper we use local three-dimensional simulations in a box in order to understand the nature of large-scale magnetic field generation. We argue that large-scale dynamo action of dynamically strong magnetic field is based on magnetic instabilities. One important consequence is that the effective α increases with increasing field strength. This behavior can possibly be verified observationally. The idea of an α-effect that increases with the magnetic field is related to previous studies suggesting that the α-effect might *not* be caused simply by cyclonic events, as originally suggested by Parker (1955), but instead by magnetically buoyant flux tubes (Leighton 1969; Schüssler 1980). We elaborate further on this approach, which comprises a whole new class of mechanisms, where the α-effect is not caused by a pre-existing flow field, but instead by the dynamics of the generated magnetic field itself. For more information about several related topics see my home page under http://antares.ncl.ac.uk/~brandenb.

2. A Dynamically Generated α-Effect

In this section we try to avoid any explicit reference to a flux tube model, except for interpretation purposes and for examining numerical results in a cartoon picture-like fashion. Instead, we focus on presenting recent simulations, where the magnetic field is crucial for driving the motions. This is in stark contrast to the traditional belief that the magnetic field would quench the motions, which generate the magnetic field. This possibility has been discussed in the past. However, it has never been shown that this can actually work. In view of Lenz' rule it seems counterintuitive to have a dynamo based on the velocity that is generated by the resulting magnetic field itself.

In his thesis, Dieter Schmitt (1985) proposed a dynamo effect based on destabilized magnetostrophic waves. He found an α-effect that was negative in lower latitudes just north of the equator, but positive in higher latitudes. Schmitt (1987) himself, and later with others (Schmitt, Schüssler & Ferriz-Mas et al. 1996), presented dynamo models based on this effect. However, in view of Lenz' rule one would really like to see evidence from simulations showing that this mechanism works and that it leads to dynamo action.

There is a related approach based on the Parker and other magnetic instabilities of flux tubes by Ferriz-Mas, Schmitt, & Schüssler (1994), where the authors find an α-effect whose sign depends on the magnetic field strength and the wave number. More recently, similar investigations have been carried out in connection with the dynamo effect in galaxies (Hanasz & Lesch 1997).

The various investigations mentioned above appear to have something in common with the simulations of accretion disk turbulence by Brandenburg et al. (1995, 1996a), where a dynamo generated magnetic field drives the turbulence owing to Balbus-Hawley and Parker instabilities. In those simulations a strong large-scale magnetic field is found. This component of the field is cyclic with a

period of 30 orbits and it shows migration away from the midplane. This field can be described by an $\alpha\Omega$-dynamo in a slab geometry, where α is negative above the midplane (and negative below), and its magnitude is roughly $1/30^2 = 10^{-3}$ times the sound speed. Before we go into these issues in more detail, let us first discuss the significance of this result.

Over the past few years various related arguments against mean-field dynamo theory have been put forward. One of the arguments was that strong fluctuations of the magnetic field would be generated from the large-scale field. Such fluctuations would limit further growth of the large-scale field (Kulsrud & Anderson 1992) to values that are smaller by a factor $R_{\rm m}^{-1/2} \approx 10^{-4}$ than the equipartition value, $B_{\rm eq} \equiv \langle 4\pi\rho\mathbf{u}^2\rangle^{1/2}$ (Vainshtein & Cattaneo 1992). Here, $R_{\rm m}$ is the magnetic Reynolds number, measuring the relative importance of field advection to magnetic diffusion. Although some of the arguments that have been presented may not be very convincing, there remains the possibility that the dynamo works in ways quite different from what has been anticipated so far. More specifically, the dynamo may not only be strongly influenced by nonkinematic effects, but it may survive into the nonlinear regime just because of those nonkinematic effects!

3. An Example of a Dynamically Generated α-Effect

We make a little excursion to accretion disks, not because they resemble stars in any obvious way, but because they provide at the moment probably one of the best examples of a numerical turbulence simulation that shows cyclic magnetic activity. The recent simulations by Brandenburg et al. (1995) were originally intended to explain the origin of self-excited turbulence in accretion disks. [Disks are linearly stable in the absence of magnetic fields, so there would be no turbulence, which is, of course, crucial for angular momentum transport. In the presence of a weak magnetic field, however, there is the linear Balbus-Hawley (1991) instability, which drives three-dimensional turbulence (Hawley, Gammie, & Balbus 1995), and which is able to reinforce the magnetic field by dynamo action (Brandenburg et al. 1995; Hawley, Gammie, & Balbus 1996; Stone et al. 1996).] The discovery of large-scale magnetic field generation in the simulations of Brandenburg et al. (1995) triggered a series of work trying to explain this in terms of mean field-type dynamo theory (Vishniac & Brandenburg 1997; Brandenburg & Donner 1997). One of the main problems is simply the sign of α: it was found to be negative in the northern hemisphere, even though the helicity of the flow has the expected (negative) sign. This then led to the realisation that the effective α in those simulations could really be due to *magnetic instabilities*, and not due to thermal convection (Brandenburg 1997).

In the simulations of Brandenburg et al. (1995) the large-scale field, especially the toroidal magnetic field component, shows remarkable spatio-temporal coherence. The field varies not only cyclically (Figure 1), but it also migrates away from the midplane (Figure 2). The traditional approach to understand such organized behavior is to adopt the mean-field approach, where the original induction equation is averaged and turbulent transport coefficients are introduced that describe the evolution of the nonlinear term, $\boldsymbol{\mathcal{E}} \equiv \langle \mathbf{u}' \times \mathbf{B}' \rangle$ in terms of the mean field itself. In principle such parameterizations can be fairly com-

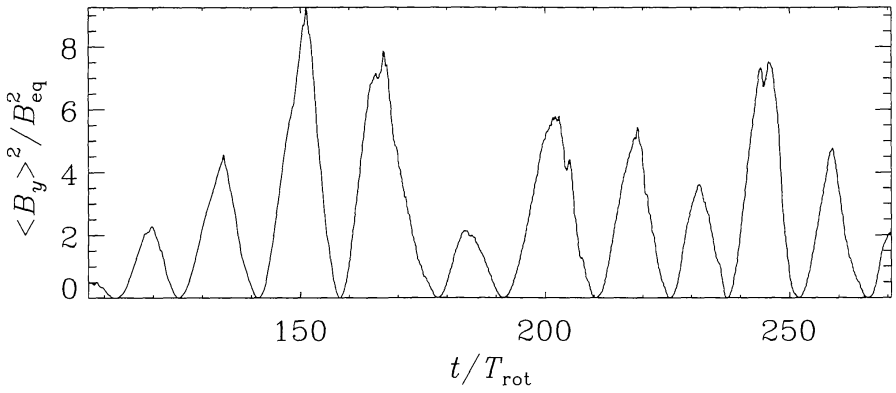

Figure 1. The square of the mean toroidal magnetic field, $\langle B_y \rangle^2$, normalized by the squared equipartition field strength, $B_{\rm eq}^2$. Note that cycle length and amplitude vary from cycle to cycle, similar to the solar cycle. The data are from Model O of the three-dimensional simulation of Brandenburg et al. (1996a).

plicated, but more importantly, they are typically extremely uncertain. We may therefore use the simulations to estimate the "transport coefficients" assuming a relation $\boldsymbol{\mathcal{E}} = \boldsymbol{\mathcal{E}}(\langle \mathbf{B} \rangle)$. Such a relation should contain terms that are capable of producing dynamo action. So, in its crudest approximation it should take the form

$$\langle \mathbf{u}' \times \mathbf{B}' \rangle = \alpha \langle \mathbf{B} \rangle - \eta_t \nabla \times \langle \mathbf{B} \rangle, \tag{1}$$

where α is the traditional dynamo α-effect and η_t is a turbulent magnetic diffusivity. The simulations are consistent with the following estimates: $\alpha \approx -0.001 \Omega H$ and $\eta_t \approx 0.008 \Omega H^2$, where Ω is the angular velocity and H the disk scale height. The sign of α is negative in the upper disk plane, but positive in the lower (southern) disk plane; see Brandenburg et al. (1995), Brandenburg & Donner (1997). This is quite peculiar: the opposite result is expected from conventional mean-field theory, where the α-effect is related the helicity of the turbulence. While the helicity of the turbulence in our simulations does have the expected sign, the simulations indicate that it has not much to do with α.

A negative α-effect has various implications. First of all, if the generated magnetic field is oscillatory, as in fact it is in the simulations, there will be a magnetic field migration associated with its cyclic variation. This is indeed what is observed in the simulations. The direction of this field migration is consistent with the implied negative sign of α.

In order to get an idea of why our α has the opposite sign we now present a rough calculation, assuming that the fluid motion is governed by magnetic buoyancy, so

$$\frac{\partial u_z'}{\partial t} = -\frac{\rho'}{\rho} g = \frac{(B^2)'}{8\pi p} g \approx \frac{\langle B_y \rangle B_y'}{4\pi p} g, \tag{2}$$

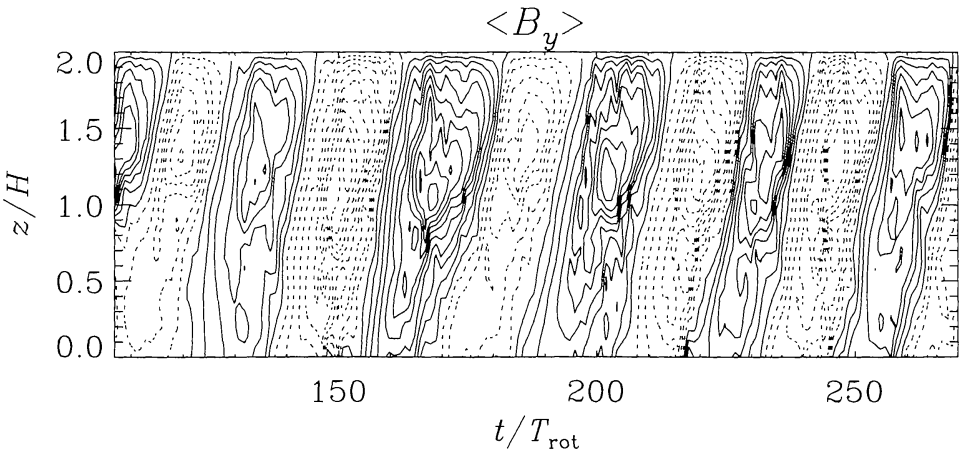

Figure 2. Spatio-temporal pattern of the toroidal component of the large-scale field, $\langle B_y \rangle$, as a function of height above the midplane of the disk and time in units of rotation periods. The data are from Model O of the three-dimensional turbulence simulation of Brandenburg et al. (1996a).

where ρ is density, p gas pressure, g gravity, and primes indicate fluctuations. As above, we have adopted a local cartesian coordinate system, where y corresponds to the azimuthal direction and x to the radial direction in cylindrical polar coordinates. The resulting electromotive force is then

$$\mathcal{E}_y = \langle u'_z B'_x - u'_x B'_z \rangle \approx \langle u'_z B'_x \rangle = +\langle B_y \rangle \frac{\langle B'_x B'_y \rangle}{4\pi p} g\tau, \tag{3}$$

where τ is some relevant time scale. Now, because of shear ($\partial u_y / \partial x < 0$) we have $\langle B'_x B'_y \rangle < 0$. Since

$$\mathcal{E}_y = \alpha_{yy} \langle B_y \rangle + ..., \tag{4}$$

we have (ignoring higher order terms)

$$\alpha_{yy} = +\langle B_y \rangle \frac{\langle B'_x B'_y \rangle}{4\pi p} g\tau. \tag{5}$$

In accretion disk theory the *negative* ratio of the horizontal Maxwell stress and the gas pressure is basically the Shakura-Sunyaev viscosity parameter $\alpha_{\rm SS}$, which we know is about 0.01 (Brandenburg et al. 1995; Stone et al. 1996), so we can write

$$\alpha_{yy} \approx -0.01 g\tau. \tag{6}$$

The effects of rotation and shear are now hidden in the fact that the stress $\langle B'_x B'_y \rangle$ is negative, which is due to the negative shear (Ω decreasing radially outwards). This estimate also assumes that the thermal expansion of buoyant tubes is small compared with the magnetic contraction due to the $\mathbf{B} \cdot \nabla \mathbf{B}$ term. Otherwise the sign may be the conventional one.

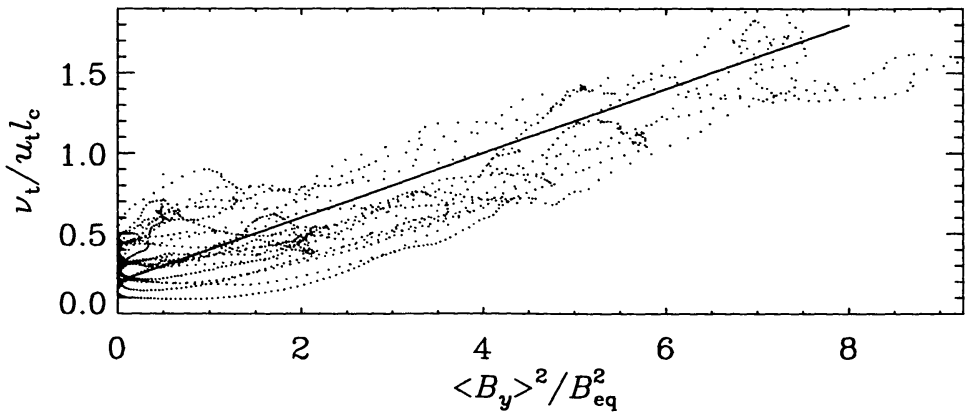

Figure 3. Turbulent viscosity as a function of the mean magnetic field. The dots refer to data obtained at different times during the simulation. The solid line gives the approximate fit formula Eq. (7).

Below we will argue that both α and η_t should increase with magnetic field strength. However, it is difficult to estimate the magnetic field dependence of those two parameters. What we can do is to calculate instead the turbulent viscosity ν_t as a function of the mean magnetic field. We find that ν_t does depend on the mean magnetic field approximately like

$$\nu_{\rm t} = 0.2 u_{\rm t} l_{\rm c} \left(1 + \langle \mathbf{B} \rangle^2 / B_{\rm eq}^2\right), \tag{7}$$

see Figure 3. Here, $u_{\rm t}$ is the turbulent root-mean-square velocity and $l_{\rm c}$ is the effective correlation length, which Brandenburg & Donner estimated to be $0.03H$ for that calculation. Since both $\eta_{\rm t}$ and $\nu_{\rm t}$ describe turbulent mixing, it is possible that $\eta_{\rm t}$ and $\nu_{\rm t}$ are related to each other simply by a constant numerical parameter (the magnetic Prandtl number). Of course, we are not sure about this, but we emphasize at this point that at least $\nu_{\rm t}$ does increase with increasing field strength.

4. Convection with Shear

What makes the simulations discussed above so distinctively non-solar is the driving of the turbulence by shear, rather than by convection. Traditional belief is that the solar dynamo is driven by convective turbulence either in the convection zone or just below it, where overshooting plumes drive the flow. In this overshoot layer shear is important for converting radial magnetic field into toroidal. There is no compelling evidence that shear contributes directly to driving the flow that is responsible for dynamo action although future simulations, where shear is included, should clarify this issue.

At the moment we only have preliminary simulations that aim at understanding the influence of shear on convective dynamo action (Brandenburg,

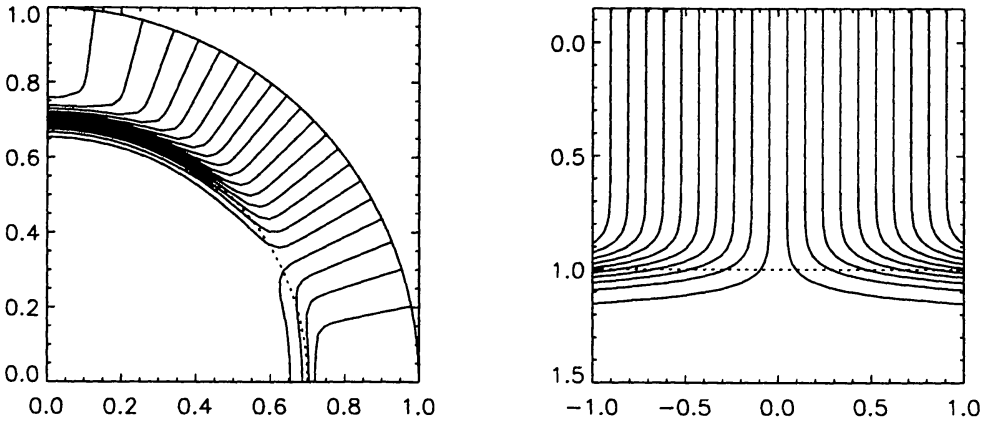

Figure 4. Idealized profiles of solar differential rotation. *Left panel*: contours of $\Omega(r,\theta)$ for the sun. *Right panel*: contours of $u_y^{(0)}(x,z)$ using (8). Note that near 30° latitude the contours of $u_y^{(0)}$ resemble those of Ω, except for some asymmetry that is absent in the cartesian model (right panel).

Nordlund & Stein 1997). Convective dynamos in local box geometry typically produce small-scale magnetic fields (Nordlund et al. 1992; Brandenburg 1996b). Owing to rotation and stratification the convective flow becomes highly anisotropic and this should drive differential rotation (Rüdiger 1989). While this can be seen in such simulations (Pulkkinen et al. 1993), the effect is smaller than it would be under more realistic circumstances, where the computational domain is not confined and where effects of spherical geometry could play a role.

Thus, it seems that local models would not be appropriate for studying differential rotation. On the other hand, since the (local) accretion disk simulations discussed above proved quite successful in producing large-scale dynamo action, it seems possible to study at least the dynamo aspect in a local model of the solar dynamo. In order to do this we have to impose however some solar-like differential rotation profile in the simulations. This can be done in a way similar to the accretion disk simulations, the difference being that the shear has to depend on height. In the deeper radiative interior of the sun there is hardly any shear, whereas in the bulk of the convection zone there is strong latitudinal shear. Thus, we use the following profile for the imposed toroidal velocity

$$u_y^{(0)}(x,z) = xf(z), \tag{8}$$

where $f(z)$ is a profile function (zero below the overshoot layer, constant and different from zero in the convection zone). The restriction to only linear latitudinal shear is essential and cannot be avoided in our particular approach (Brandenburg et al. 1995), where the shearing box approximation is made, i.e., pseudo-periodic boundary conditions are used.

In Figure 4 we compare an idealized profile of solar differential rotation with (8). In the plot of $u_y^{(0)}(x,z)$ where we have used $f(z) = \frac{1}{2}(1-\tanh\frac{z-z_0}{d_0})$, $z_0 = 1$,

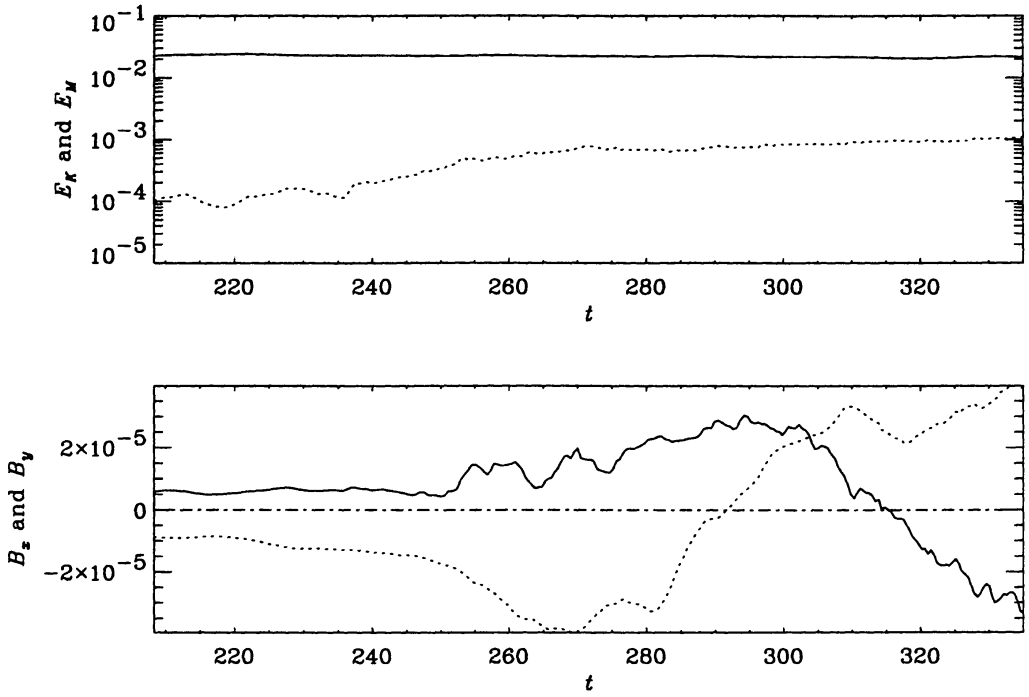

Figure 5. *Upper panel*: Evolution of kinetic and magnetic energies (solid and dotted lines). *Lower panel*: Evolution of mean radial and toroidal fields (dotted and solid lines).

$d_0 = 0.1$. The (preliminary!) simulations indicate an evolution of the mean magnetic field components in the horizontal directions, $\langle B_x \rangle$ and $\langle B_y \rangle$. Figure 5 seems to show the beginning of a solar cycle. It is remarkable that $\langle B_x \rangle$ and $\langle B_y \rangle$ seem to show a $3\pi/4$ phase shift in a similar manner as the accretion disk simulation (Brandenburg et al. 1996a).

5. Observations

Let us now look at observed stellar cycle data. Although stellar cycle data have been looked at many times in the past (Noyes, Weiss, & Vaughan 1984; Baliunas & Vaughan 1985; Baliunas, Sokoloff, & Soon 1996; Baliunas et al. 1996), we feel that a fresh look at things could be helpful, especially if we have to ask new questions, for example: can we learn anything about the dependence of α on field strengh? Using now the stellar cycle periods, $P_{\rm cyc}$, published by Baliunas et al. (1995), the rotation periods, $P_{\rm rot}$, and the normalized chromospheric activity measure, $\langle R'_{\rm HK} \rangle$, from Donahue, Saar, & Baliunas (1996) we have plotted all possible correlations between

- the ratio of cycle and rotation frequencies, ω/Ω,
- the inverse Rossby number, Ro^{-1},

- the mean activity level, $\langle R'_{\rm HK}\rangle$, and
- the spectral type, measured by color index $B-V$.

Here, $\omega = 2\pi/P_{\rm cyc}$, $\Omega = 2\pi/P_{\rm rot}$, and ${\rm Ro}^{-1} = 2\Omega\tau_{\rm c}$, where $\tau_{\rm c}$ is the turnover time. We have adopted the 'empirical' turnover time of Noyes et al. (1984). The result is shown in Figure 6. In this plot we have taken only those stars for which the 'false alarm probability' is large enough (with grades good and excellent). Furthermore, in those cases where two periods have been reported, we always take the longer one of the two. A full account of this work is in preparation together with Steve Saar and Chris Turpin.

There are three plots that show systematic behavior. There is first of all the plot of $\langle R'_{\rm HK}\rangle$ against ${\rm Ro}^{-1}$, which shows an approximately linear behavior in the parameter range covered by all the cyclic stars with well-defined cycles. This plot is basically consistent with a similar plot by Noyes et al. (1984). Secondly, the plot of the ratio ω/Ω against $\langle R'_{\rm HK}\rangle$ shows two separate branches, an upper one for small values of $\langle R'_{\rm HK}\rangle$ (corresponding to inactive stars) and a lower one for large values of $\langle R'_{\rm HK}\rangle$ (corresponding to active stars). Soon, Baliunas, & Zhang (1993) have discussed a similar plot, where $\langle R'_{\rm HK}\rangle$ was used as an age indicator. The segregation of cycle periods was first discussed by Saar & Baliunas (1992). From the two correlation plots in panels c and d it follows that ω/Ω versus ${\rm Ro}^{-1}$ must also show a correlation, which is does. However, the scatter in that third plot is somewhat larger than in the previous two plots. The dashed slope in that plot is not a least square fit to the data, but it is the correlation inferred from the previous two plots.The remaining three plots in Figure 6 involving $B-V$ show no correlation. From panels b-d we obtain approximate powerlaw fits

$$\omega/\Omega = c_1 {\rm Ro}^{-\sigma} \quad \text{(Figure 6b)}, \tag{9}$$

$$\omega/\Omega = c_2 \langle R'_{\rm HK}\rangle^{\nu} \quad \text{(Fig. 6c)}, \tag{10}$$

$$\langle R'_{\rm HK}\rangle = c_3 {\rm Ro}^{-\mu} \quad \text{(Fig. 6d)}. \tag{11}$$

Note that Eq. 9 can be derived from equations (10) and (11), with

$$c_1 = c_2 c_3^{\nu}, \quad \sigma = \mu\nu. \tag{12}$$

The scaling exponents σ, ν and μ are given in Table 1 separately for active and inactive stars.

Table 1. List of scaling exponents found from the fit shown in panels Figure 6c and Figure 6d. Note that σ is calculated from μ and ν using Eq. (12).

	inactive	active
σ	0.81	0.57
ν	0.83	0.58
μ	0.98	0.98

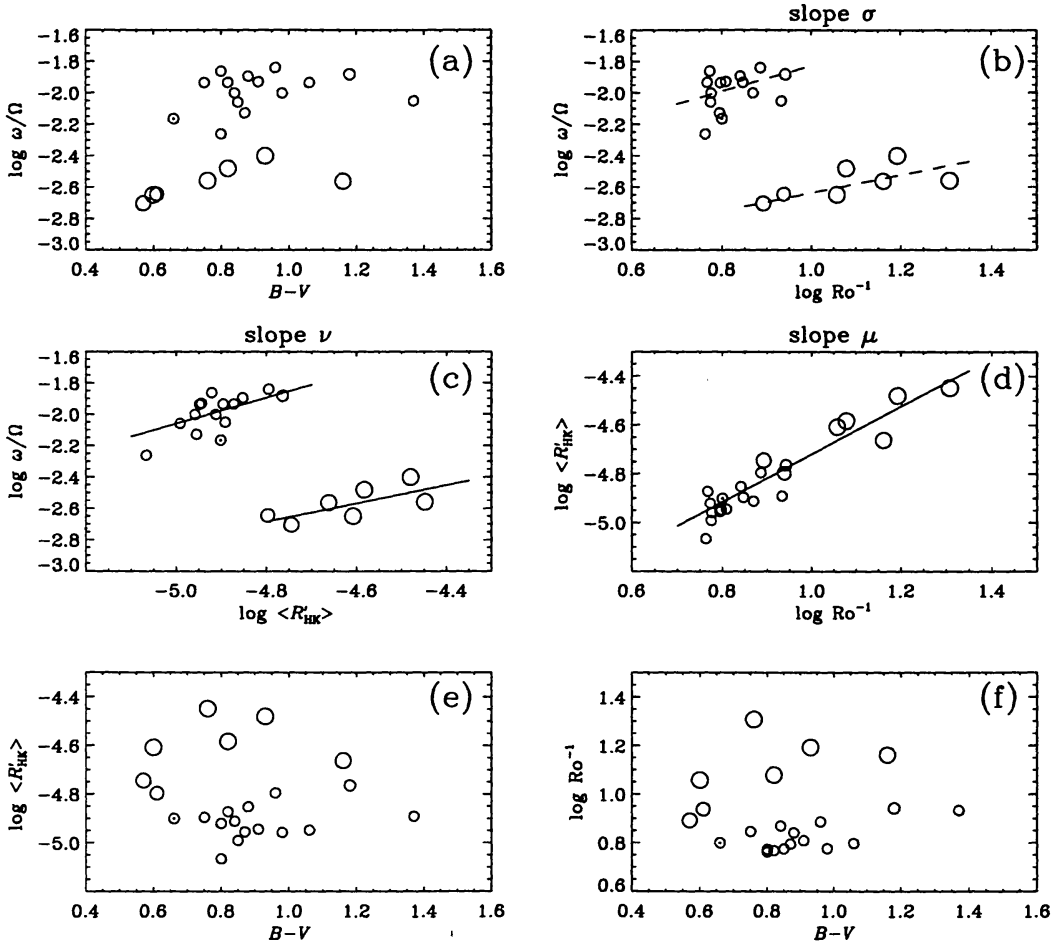

Figure 6. Correlation of all six possible combinations of the four parameters ω/Ω, Ro^{-1}, $\langle R'_{\rm HK}\rangle$, and $B-V$. Young and active stars are represented by larger symbols. In panels (c) and (d) we give least square fits separately for active and inactive stars. The dashed lines in panel (b) give the dependence implied by the fits for panels (c) and (d).

6. Comparison with a Simple Nonlinear Dynamo Model

We now consider a very simple model, which has the advantage that we can derive exact relations between the type of nonlinear terms in the equations and the behavior of the solutions. Using the standard $\alpha\Omega$ dynamo equations (Parker 1979) one can show that there is a wave-like solution. In a local approximation this so-called Parker dynamo wave is governed by the equation

$$\dot{A} = \alpha B - \eta k^2 A, \tag{13}$$

$$\dot{B} = ikL\Omega' A - \eta k^2 B, \tag{14}$$

where Ω' is the vertical gradient of the angular velocity, k is the wave vector in the latitudinal direction, the parameter α describes the α-effect, and L is a typical length scale for the star. Following Durney & Robinson (1983), we assume k to be fixed and introduce the diffusion time $\tau = (\eta k^2)^{-1}$, so we have

$$\dot{A} = \alpha B - \tau^{-1} A, \tag{15}$$

$$\dot{B} = ikL\Omega' A - \tau^{-1} B. \tag{16}$$

In the linear case, when α and τ are independent of A and B, the solution is of the form $B \sim \exp(\lambda t - i\omega t)$, where

$$\lambda = \pm|\alpha\Omega' kL/2|^{1/2} - \tau^{-1}, \tag{17}$$

$$\omega = \pm|\alpha\Omega' kL/2|^{1/2}, \tag{18}$$

i.e., the frequency ratio is proportional to the square root of α. In what follows the normalized cycle frequency, ω/Ω, will be of some interest. It is given by

$$\frac{\omega}{\Omega} = \pm\left|\frac{\alpha}{\Omega L}\frac{\Omega' L}{\Omega}\frac{kL}{2}\right|^{1/2}. \tag{19}$$

Assuming that $\Omega' L/\Omega$ and $kL/2$ are of order unity we have

$$\omega/\Omega \approx \pm\,|\alpha/\Omega L|^{1/2}. \tag{20}$$

We are interested in solutions that are saturated by some nonlinear process. It is often assumed that α decreases with increasing field strength. However, from this it follows directly that the normalized cycle frequency ω/Ω decreases with increasing field strength. In fact, we have seen in Figure 6c that, except for a jump at $\log\langle R'_{\rm HK}\rangle \approx -4.7$, the opposite is actually observed. Therefore we allow for the possibility that α increases with increasing field strength; see Figure 7. This possibility is supported by the recent realisation that the α effect could be due to the magnetic field itself (Ferriz-Mas et al. 1994; Brandenburg & Donner 1997), rather than due to convection (Parker 1955; Krause & Rädler 1980). No other mechanism is currently known that would lead to an increase of ω/Ω with Ro^{-1}; see also Rüdiger & Arlt (1996).

We assume now that α and τ^{-1} depend on the field strength in the following way

$$\alpha = \alpha_0 + \alpha_1 |B/B_0|^n, \tag{21}$$

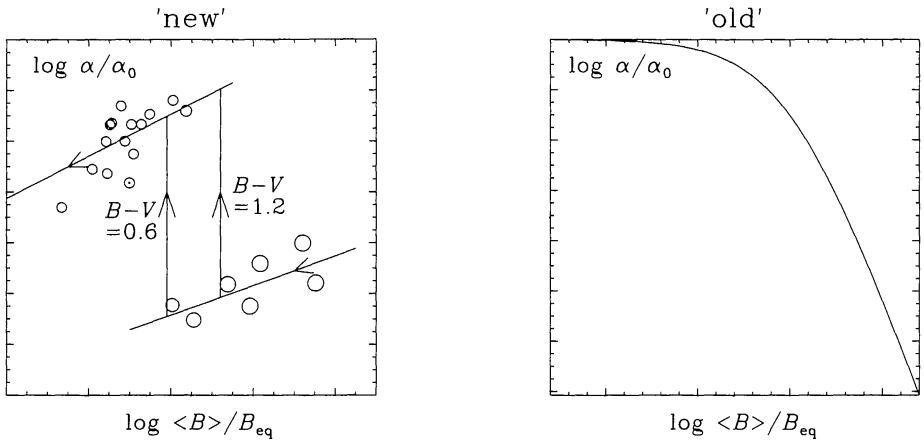

Figure 7. Comparison of the new $\alpha(B)$ dependence inferred from the observations (left hand panel) with the old α-quenching curves of the form $\sim 1/(1+\langle\mathbf{B}\rangle^2)$, which is here shown in a double-logarithmic plot. As stars get older, the magnitude of $\langle\mathbf{B}\rangle$ decreases, and so they evolve in this plot to the left. At some field strength, which depends on the spectral type, i.e., on $B-V$, the star jumps onto the upper branch, which is governed by a different type of magnetic instability causing the α-effect. This is quite different from the conventional concept of α-quenching.

$$\tau^{-1} = \tau_0^{-1} + \tau_1^{-1}|B/B_0|^m. \tag{22}$$

For negative exponents α and τ^{-1} go singular near $B \to 0$, but we shall not be concerned with this limit. The asymptotic behavior for large values of B (or in the limit $\alpha_0 = \tau_0^{-1} = 0$) is governed by a balance between generating terms, $(\alpha_1\Omega' kL/2)^{1/2}|B/B_0|^{n/2}$ and dissipating terms, $\tau_1^{-1}|B/B_0|^m$. It is convenient to define the dimensionless quantity

$$S = \frac{\alpha_1}{\Omega}\frac{\Omega'}{\Omega}\frac{kL}{2}. \tag{23}$$

The functional dependence of α_1 and Ω' is unclear, but it is likely that they depend on the geometry and in particular on the depth of the convection zone, i.e., on the spectral type. The dependence of S on Ω is possibly weak, so as a first approximation we may assume S to be independent of Ω. We also define the Rossby number,

$$\mathrm{Ro} = (2\Omega\tau)^{-1}, \tag{24}$$

where τ is now approximated by τ_1. In terms of those two dimensionless numbers the balance between generation and dissipation in Eq. (17) can we written as $0 = S^{1/2}|B/B_0|^{n/2} - 2\mathrm{Ro}|B/B_0|^m$, or

$$(B/B_0)^{1/2} = 2^{-\mu}S^{\mu/2}\mathrm{Ro}^{-\mu}, \quad \text{where} \quad \mu = \frac{1}{2m-n}. \tag{25}$$

Here we consider the square root of the magnetic field, because Schrijver et al. (1989) have shown that the chromospheric emission parameter $\langle R'_{\rm HK}\rangle$ is roughly proportional to the square root of the magnetic field.

The normalized cycle frequency is $\omega/\Omega = (\alpha_1 \Omega' k L/2)^{1/2} |B/B_0|^{n/2}$, or

$$\omega/\Omega = S^{1/2}(B/B_0)^{\nu}, \quad \text{where} \quad \nu = n/2. \tag{26}$$

From Eqs. (25) and (26) we can eliminate B/B_0 and obtain

$$\omega/\Omega = 2^{\sigma} S^{(\sigma+1)/2} {\rm Ro}^{-\sigma}, \quad \text{where} \quad \sigma = \mu n = \frac{n}{2m-n}. \tag{27}$$

In Table 2 we give the results for μ, σ and ν for different (plausible?) combinations of n and m.

Table 2. Results for μ, σ and ν for different combinations of n and m.

n	m	μ	σ	ν
-2	0	1/2	-1	$-1/2$
0	2	1/4	0	0
1	1	1	1	1/2
1	2	1/3	1/3	1/2
1	3	1/5	1/5	1/2
2	2	1/2	1	1
2	4	1/6	1/3	1

The parameters μ, ν and σ are in principle the same parameters as the observable scaling exponents introduced earlier and listed in Table 1. Thus, the measured values of μ, ν and σ could be used to determine the exponents n and m via

$$n = 2\nu, \quad m = \nu + (2\mu)^{-1}. \tag{28}$$

In all cases the dependence on B has to be identified with a dependence on $\langle R'_{\rm HK}\rangle$ (Schrijver et al. 1989). The result is shown in Table 3.

Table 3. Summary of the theoretically inferred parameters n and m.

	inactive	active
n	1.66	1.16
m	1.34	1.09

At this point we do not know whether those values are consistent with theory. The simulations suggest a quadratic increase in ν_t, and if $\nu_t = \eta_t$ this would mean $m = 2$, instead of 1.34 and 1.09 for inactive and active stars, respectively. On the other hand, the model is too simple, and preliminary calculations of two-dimensional dynamo models suggest that the assumption of a single mode does not hold; see also Tobias (1997) and the comments made during the discussion.

7. Conclusions

The observations point toward the possibility that the field generating effect increases with increasing field strength. The early semi-empirical model by Leighton (1969) had already the property of an α-effect that increased with increasing field strength. However, in his model he used a step function, so α was zero below some critical field strength, but nonzero and constant above. In order to have field saturation the dissipative effects must also increase with increasing field strength. MHD simulations point in a similar direction. Those results are in line with previous attempts to explain the solar dynamo in terms of buoyant magnetic flux tubes (Schüssler 1980). More recent work in that direction has been carried out by Ferriz-Mas et al. (1996), but in that work only modes of low azimuthal order (with azimuthal wave numbers $m = 1$ and $m = 2$) are the dominant contributors, which seems rather low and one would not really call that turbulence.

The instabilities identified in the present work include magnetic shearing and buoyancy instabilities. However, there are other candidates that may be more appropriate for the sun. There are first of all the magnetostrophic waves studied by Schmitt (1985). In that case the waves were destabilized by having B/ρ decrease with height, which makes the system Rayleigh-Taylor unstable. Another magnetic instability studied recently in connection with the sun has been discovered by Gilman & Fox (1997). Again only a low order azimuthal mode ($m = 1$) leads to instability, which is not exactly what we have in mind when we talk about an α-effect that increases with increasing field strength. Nevertheless, the simulations indicate that a dynamo works. It is not clear that the generating effect increases really with increasing field strength, but we know that at least the dissipative effects do increase with increasing field strength. In any case, it seems that we are now somewhat at a turning point where we have to develop a new basis for the old mean field-type dynamo approach. Simulations prove a valuable tool, and their results can often be parameterized in terms of an α-effect. The nature of the α-effect is possibly quite different from what it used to be. In particular, it is probably not quenched, but it may instead be enhanced by the magnetic field.

Acknowledgments. I am grateful to Steve Saar and Chris Turpin for their contributions to the work presented in §5., and for the interesting discussions we had.

Discussion

Mark Giampapa: You have interpreted observed correlations with $R'_{\rm HK}$ as correlations with field *strength*. However, observational work suggests that surface field strengths in active and inactive stars are quite similar but differ mainly in filling factor, i.e., the magnetic surface *flux*. How does this influence your scalings of α with B?

Axel Brandenburg: You are right; I should have been more careful about this. I think what matters for the dynamo is in fact the magnetic flux, fB, and not the magnetic field strength, B. At least at the surface B is always comparable

to $\sqrt{8\pi p}$, where p is the gas pressure, so gas and magnetic pressures balance each other. The thing which changes with changing activity level is therefore fB, which is more like the mean field used in the mean-field dynamo. So, in what I presented B should therefore be replaced by fB. The anticipated scaling results do not change therefore. Just recently Steve Saar reminded me that the relation by Schrijver et al. (1989), used in Eq. (25), is actual one between Ca II surface flux and magnetic flux, and is thus of the form $F_{\rm HK} \propto (fB)^{0.5}$ (for stars below the saturation limit). However, he told me that a very similar relation also exists for the *normalized* Ca II and magnetic fluxes. Using the best currently available data for G and K dwarfs (Saar 1996) and $\sqrt{8\pi p}$ from Kurucz (1991) models (see Bünte & Saar 1993), Saar (1997, private communication) finds the relation $R'_{\rm HK} \propto (fB/B_{\rm eq})^{0.47}$, which is basically the relation needed in Eq. (25).

Carole Jordan: Since you seem have a theoretical prediction which fits observational results, am I correct in assuming that your theory explains the early empirical relation between $F'_{\rm HK}$ and Ro found by Noyes et al. (1984)? Or have you found values of parameters in theory *using* the observational results?

Axel Brandenburg: It is the latter; I have used the observational scaling results to infer the scaling properties of the α-effect and magnetic buoyancy. Theoretically we expect α to go up with increasing field strength, but we don't know how fast (i.e., does α increase proportionally with B^2, or only with $|B|$, for example). Apart from the relation between the normalized magnetic field (or rather the flux), $\langle R'_{\rm HK}\rangle$, and inverse Rossby number (Noyes et al. 1984), we also used a relation between $\langle R'_{\rm HK}\rangle$ and the ratio between cycle to rotation frequencies, which hasn't received much attention in the past. The latter shows two branches, separately for active and inactive stars. The cycle data studied for example by Noyes, Weiss, & Vaughan (1984) were only for inactive stars. To my knowledge, Saar & Baliunas (1992) were the first to draw attention to the two branches for the cycle periods.

Steven Tobias: I have a comment and a question. The comment: this joint instability is very interesting and it indicates that if only spherical simulations could reproduce the differential rotation profiles then we would have every hope of simulating the dynamo. The question: you use a 1 mode travelling wave model to relate your ideas to observations. However, recent simulations (Tobias 1997, preprint) show that the inclusion of latitudinal boundaries introduces higher modes and can lead to different conclusions about the behavior of cycle periods and rotation rate. Can you comment on the robustness of your results to the inclusion of higher modes?

Axel Brandenburg: You are right, the simple one-mode model produces a different scaling than a two-dimensional dynamo model. Unfortunately, two-dimensional calculations with an α-effect that increases with increasing field strength haven't been carried out yet. The main motivation for using the one-mode model was to illustrate a possible solution of how to explain an ω/Ω-ratio that increases with B. More realistic models need to be considered now. Maybe one can still use the one-mode model, but then S, which is proportional to the wave number k, could become a function of Ro^{-1}. So, for example, if we assume $S = S_0 \mathrm{Ro}^{-q}$,

then the new relations between n, m, μ, ν and σ are

$$\mu = \frac{1+q/2}{2m-n}, \quad \sigma = \frac{n+qm}{2m-n}, \quad \nu = \frac{n+qm}{2+q},$$

where q has to be determined by fitting the one-mode model to the results of a two-dimensional numerical dynamo calculation.

Dieter Schmitt: If the dynamo α increases with magnetic strength, what do you think limits the growth of the magnetic field?

Axel Brandenburg: Everything but α-quenching would probably do. In the present work I have considered the effect of buoyancy, as described by a flux loss term of the form $-B/\tau$ in the induction equation. Another possible mechanism could be feedback from the large-scale motions, that are generated by the magnetic field (cf. Brandenburg et al. 1992).

Ilkka Tuominen: What are the Reynolds numbers and other characteristic parameters in the simulations you presented, and how does this compare with the sun?

Axel Brandenburg: The Reynolds number Re is a few hundred (up to one thousand in some cases), the Rayleigh number Ra is between 10^6 and 10^7, and the magnetic Prandtl number $\mathrm{Pr_M} = \nu/\eta$ is between 0.5 and 4. In the sun, typical values are $\mathrm{Re} = 10^{12}$, $\mathrm{Ra} = 10^{24}$, and $\mathrm{Pr_M} = 10^{-7}$. In that sense we are thus far off from the sun. However, as far as the large scale dynamics is concerned, we hope that the results are not very sensitive to the values of the viscosity and the magnetic diffusivity, which are expressed by Re and $\mathrm{Pr_M}$ in nondimensional ways. Basically, a larger Reynolds number means that smaller scale motions are present and that the power spectrum extends to higher wave numbers. However, the large scales remain unaffected by this. To some extent we have been able to verify this in our simulations as well. The quantity that matters most is probably the resulting inverse Rossby number. In the sun we have $\mathrm{Ro}^{-1} \approx 5$, and this is similar to the value used in the simulations.

Gibor Basri: Can you comment on what will happen when you go to fully convective stars? Should there be a change in behavior?

Axel Brandenburg: I could only speculate on that. Observations tell us already that the activity does not go down as stars become fully convective, although the type of magnetic field configuration might change. Theoretically, the absence of an overshoot layer may not be crucial. Simulations have shown us that convection has a tendency to pump magnetic fields downward ('turbulent pumping'). In a fully convective star, fields will thus be pumped toward the center, where they will accumulate. It is not quite clear how the differential rotation will look like in those stars. Theory points towards surface differential rotation similar to that of the sun. If the Ω-contours were to continue inward in a spoke-like fashion, there must be some sort of a tachocline very near the center. So, basically I would expect that in a fully convective star the center region will play a role similar to the overshoot layer in other late-type stars. I don't think that flux 'storage' is a problem, because very near the center gravity is very weak, so there won't be much buoyancy.

Ed DeLuca: Flux emergence calculations suggest that the field strength near the base up to the overshoot region is as large as, or much larger than, the equipartition field strength. Are your simulations consistent with these results?

Axel Brandenburg: The magnetic field in flux tubes has to be considered as part of the fluctuating (small-scale) component of the magnetic field. The simulations show that the magnetic field fluctuations can well exceed the equipartition field strength by a factor of ten. I think the flux emergence calculations suggest field strength of around $60 - 160\,\mathrm{kG}$ for the sun, which is 10-20 times the equipartion field strength. So I think that is maybe not a big problem, although the simulations don't reach those values at the moment. However, it is important to realize that, if the magnetic field is really caused by a dynamically generated α-effect, the equipartition value does not really matter at all. For example, in the accretion disk calculations there would be no turbulence in the absence of a field. Therefore one has a zero equipartion value in that sense, and yet, strong large-scale magnetic fields can be generated.

Andrew Collier Cameron: The relation for ω/Ω derived from your simple nonlinear dynamo model incorporates a quantity Ω' representing differential rotation. What assumption have you made about the relation between Ω' and Ω?

Axel Brandenburg: I have assumed that the ratio Ω'/Ω is constant. In fact, it is possible to include a dependence of the form $\Omega'/\Omega \propto \mathrm{Ro}^{-\lambda}$, for example. This would lead to a dependence $S = S_0 \mathrm{Ro}^{-q}$, which would change the relations between n, m, μ, ν and σ, as described above. Donahue, Saar, & Baliunas (1996) find observational evidence for $\lambda \approx -0.3$.

References

Balbus, S.A., & Hawley, J.F. 1991, ApJ, 376, 214

Baliunas, S.L., & Vaughan, A.H. 1985, ARA&A, 23, 379

Baliunas, S.L., Donahue, R.A., Soon, W.H., et al. 1995, ApJ, 438, 269

Baliunas, S.L., Nesme-Ribes, E., Sokoloff, D., & Soon, W.H. 1996, ApJ, 460, 848

Baliunas, S.L., Sokoloff, D., & Soon, W.H. 1996, ApJ, 457, L99

Brandenburg, A. 1997, Acta Astron. Geophys. Univ. Comenianae, XIX, 235

Brandenburg, A., & Donner, K.J. 1997, MNRAS, 288, L29

Brandenburg, A., Moss, D., & Tuominen, I. 1992, A&A, 265, 328

Brandenburg, A., Nordlund, Å., & Stein, R.F. 1997, in preparation

Brandenburg, A., Nordlund, Å., Stein, R.F., & Torkelsson, U. 1995, ApJ, 446, 741

Brandenburg, A., Nordlund, Å., Stein, R.F., & Torkelsson, U. 1996a, ApJ, 458, L45

Brandenburg, A., Jennings, R.L., Nordlund, Å., Rieutord, M., Stein, R.F., & Tuominen, I. 1996b, J. Fluid Mech., 306, 325

Bünte, M., & Saar, S.H. 1993, A&A, 271, 167

Donahue, R.A., Saar, S.H., & Baliunas, S.L. 1996, ApJ, 466, 384

Durney, B.R., & Robinson, R.D. 1982, ApJ, 253, 290

Ferriz-Mas, A., Schmitt, D., & Schüssler, M. 1994, A&A, 289, 949

Gilman, P.A. 1983, ApJS, 53, 243

Gilman, P.A., & Fox, P.A. 1997, ApJ, 484, 439

Glatzmaier, G.A. 1985, ApJ, 291, 300

Hanasz, M., & Lesch, H. 1997, A&A, 321, 1007

Hawley, J.F., Gammie, C.F., & Balbus, S.A. 1995, ApJ, 440, 742

Hawley, J.F., Gammie, C.F., & Balbus, S.A. 1996, ApJ, 464, 690

Krause, F., & Rädler, K.-H., Mean-Field Magnetohydrodynamics and Dynamo Theory (Berliin: Akademie-Verlag); also (Oxford: Pergamon Press)

Kulsrud, R.M., & Anderson, S.W. 1992, ApJ, 396, 606

Kurucz, R.L. 1991, in Precision Photometry: Astrophysics of the Galaxy, eds. P. Davis, A. Upgren & K. Janes (Schenectady: L. Davis Press), 27

Leighton, R.B. 1969, ApJ, 156, 1

Moffatt, H. K. 1978, Magnetic Field Generation in Electrically Conducting Fluids (Cambridge: Cambridge Univ. Press)

Nordlund, Å., Brandenburg, A., Jennings, R.L., Rieutord, M., Ruokolainen, J., Stein, R.F., & Tuominen, I. 1992, ApJ, 392, 647

Noyes, R.W., Hartmann, L., Baliunas, S.L., Duncan, D.K., & Vaughan, A.H. 1984, ApJ, 279, 763

Noyes, R.W., Weiss, N.O., & Vaughan, A.H. 1984, ApJ, 287, 769

Parker, E.N. 1955, ApJ, 122, 293

Parker, E.N. 1979, Cosmical Magnetic Fields (Oxford: Clarendon Press)

Pulkkinen, P., Tuominen, I., Brandenburg, A., Nordlund, Å., & Stein, R.F. 1993, A&A, 267, 265

Rüdiger, G. 1989, Differential Rotation and Stellar Convection: Sun and Solar-Type Stars (New York: Gordon & Breach)

Rüdiger, G., & Arlt, R. 1996, A&A, 316, L17

Rüdiger, G., & Brandenburg, A. 1995, A&A, 296, 557

Saar, S.H. 1996, in IAU Colloquium 153, Magnetodynamic Phenomena in the Solar Atmosphere — Prototypes of Stellar Magnetic Activity, eds. Y. Uchida, T. Kosugi, & H.S. Hudson (Dordrecht: Kluwer), 367

Saar, S.H., & Baliunas, S.L. 1992, in ASP Conf. Ser. 27, The Solar Cycle, ed. K.L. Harvey (San Francisco: ASP), 150

Schmitt, D. 1985, Dynamowirkung Magnetostrophischer Wellen, PhD dissertation, University of Göttingen

Schmitt, D. 1987, A&A, 174, 281

Schmitt, D., Schüssler, M., & Ferriz-Mas, A. 1996, A&A, 311, L1

Schrijver, C.J., Cote, J, Zwaan, C., & Saar, S.H. 1989, ApJ, 337, 964

Schüssler, M. 1980, Nature, 288, 150

Soon, W.H., Baliunas, S.L., & Zhang, Q. 1993, ApJ, 414, L33

Stone, J.M., Hawley, J.F., Gammie, C.F., & Balbus, S.A. 1996, ApJ, 463, 656

Tobias, S. 1997, MNRAS, in press.
Vainshtein, S.I., & Cattaneo, F. 1992, ApJ, 393, 165
Vishniac, E. T., & Brandenburg, A. 1997, ApJ, 475, 263